Zeitschrift: IABSE reports of the working commissions = Rapports des commissions de travail AIPC = IVBH Berichte der Arbeitskommissionen

Band: 29 (1979)

Artikel: Nonlinear dynamic analysis of reinforced concrete slabs

Autor: Sinisalo, H.S. / Tuomala, M.T.E. / Mikkola, M.J.

DOI: https://doi.org/10.5169/seals-23559

IV

Nonlinear Dynamic Analysis of Reinforced Concrete Slabs

Analyse dynamique non linéaire des plaques en béton armé

Nichtlineare dynamische Analyse von Stahlbetonplatten

H.S. SINISALO
Research Assistant
Helsinki University of Technology
Espoo, Finland

M.T.E. TUOMALA
Research Assistant
Helsinki University of Technology
Espoo, Finland

M.J. MIKKOLA
Research Professor
Helsinki University of Technology
Espoo, Finland

SUMMARY

The paper is concerned with the analysis of reinforced concrete slabs subjected to transient impulsive loading. Tensile cracking, the plastic behaviour of concrete in multiaxial state of stress and the plastic deformation of the reinforcement are taken into account. Geometrical nonlinearity is included. The plate theories of Kirchhoff and Mindlin are used. The problem is discretized spatially and temporally by use of the finite element and finite difference methods, respectively. Some static and dynamic problems of slabs are analyzed and the results compared with experimental and numerical data obtained elsewhere.

RESUME

Cet article traite de l'analyse des plaques en béton armé soumises à des charges transitoires et impulsives. La fissuration, le comportement plastique du béton dans un état multiaxial de contrainte et la déformation plastique des armatures sont prises en considération. Les nonlinéarités géométriques sont considérées. Les théories de Kirchhoff et de Mindlin sont utilisées. Le problème est rendu discret spatialement et temporellement par les méthodes des éléments finis et des différences finies. Quelques problèmes statiques et dynamiques sont étudiés et les résultats comparés avec des résultats numériques et expérimentaux obtenus ailleurs.

ZUSAMMENFASSUNG

Die vorliegende Arbeit befasst sich mit der Analyse von impulsartig belasteten Stahlbetonplatten. Die Rissbildung im Zugbereich, die plastischen Deformationen des Betons unter dem mehrachsigen Spannungszustand und die plastischen Dehnungen der Stahlstäbe werden berücksichtigt. Geometrische Nichtlinearitäten werden ebenfalls berücksichtigt. Die Plattentheorien von Kirchhoff und Mindlin werden verwendet. Die Diskretisierung des Problems erfolgt räumlich nach der Finite Elemente Methode und zeitlich nach der Differenzenmethode. Einige statische und dynamische Plattenprobleme werden berechnet, und die Ergebnisse werden mit experimentellen und numerischen Resultaten anderer Untersuchungen verglichen.

1. INTRODUCTION

In problems of reactor safety and protective structures extreme dynamic loads can be encountered, and for safe and economic design the nonlinear behaviour of the material and the structure has to be considered. Major sources of nonlinearity in reinforced concrete structures are the progressive cracking in tension, the nonlinear response of reinforcing steel in tension and of concrete under compression, and other nonlinearities related to reinforcement and its interaction with concrete. In sudden loading the effect of high strain rate on the behaviour of concrete and steel should also be accounted for.

The finite element method has enabled the solution of the complicated problems represented by the nonlinear behaviour of reinforced concrete structures. Several studies on the nonlinear behaviour of reinforced concrete structures subjected to static loads have been published in recent years, see [1-6] and others. On the other hand, only few reports on dynamic analysis of reinforced concrete are available [7-12].

The purpose of this paper is to report on the study of reinforced concrete slabs subjected to transient impulsive loading. In initial state, elastic behaviour is assumed for the composite material formed by concrete and reinforcement. Tensile cracking of the concrete and the plastic behaviour of the concrete in biaxial compression and of the reinforcing steel are taken into account. The reinforcement is described as smeared and orientated steel layers. The equation of motion is derived using the principle of virtual displacements in total Lagrangian approach. The kinematic equations of plates are taken in accordance with the theories of Kirchhoff and Mindlin. The problem is discretized spatially and temporally by use of the finite element and finite difference methods, respectively. Some static and dynamic problems of slabs are analyzed and the results compared with available experimental or numerical values.

2. KINETIC AND KINEMATIC EQUATIONS

In total Lagrangian approach the pronciple of virtual displacements can be written in the form [13]

$$\int_{V_o} S\delta E dV - \int_{V_o} f\delta u dV - \int_{A_t} t\delta u dA + \int_{V_o} \rho\ddot{u}\delta u dV = 0 \qquad (1)$$

where S is the 2nd Piola-Kirchhoff stress, E the Green-Lagrange strain, f and t the prescribed body force and surface traction, respectively, ρ the density, u the displacement, and $\ddot{u}$ the acceleration. V_o denotes the initial volume of the body and A_t the part of the initial boundary on which the traction is given. The use of finite element approximation $u = Nq$ results in matrix equation

$$R(q) + M\ddot{q} = Q \qquad (2)$$

where q is the vector of nodal displacements, and

$$R = \int_{V_o} B^T S dV, \qquad Q = \int_{V_o} N^T f dV + \int_{A} N^T t dA, \qquad M = \int_{V_o} N^T \rho N dV \qquad (3)$$

are the force of internal stresses, the load vector, and the mass matrix, re-

spectively. The matrix B, dependent on the current state, is defined by the strain variation $\delta E = B\delta q$. The incremental form of the equation of motion (2) is

$$ {}^{1}K_t \Delta q + M\ddot{q} = {}^{2}Q - {}^{1}R \tag{4} $$

where

$$ {}^{1}K_t = \int_{V_o} {}^{1}B^T {}^{1}D\, {}^{1}B \, dV \tag{5} $$

is the tangent stiffness matrix. Left superscripts 1 and 2 refer to the configurations of the body at times t and $t + \Delta t$, respectively. The constitutive matrix D relates the stress and strain rates, $\dot{S} = D\dot{E}$.

In Mindlin's thick plate theory, the assumption is made that normals to the midplane remain straight but not necessarily normal to the midsurface after deformation. The nonlinear strain-displacement relation can be written in the form [14]

$$ \begin{Bmatrix} \varepsilon_x \\ \varepsilon_y \\ \gamma_{xy} \\ \gamma_{xz} \\ \gamma_{yz} \end{Bmatrix} = \begin{Bmatrix} u_{,x} + w_{,x}^2/2 \\ v_{,y} + w_{,y}^2/2 \\ u_{,y} + v_{,x} + w_{,x} w_{,y} \\ w_{,x} + \varphi \\ w_{,y} + \psi \end{Bmatrix} + z \begin{Bmatrix} \varphi_{,x} \\ \psi_{,y} \\ \varphi_{,y} + \psi_{,x} \\ 0 \\ 0 \end{Bmatrix} \tag{6} $$

where u and v are the in-plane displacements and w the deflection of the midplane and φ and ψ represent the rotations of the normal with respect to x-and y-axes. The corresponding relationships of the thin plate theory of Kármán-Kirchhoff are obtained by setting $\varphi = -w_{,x}$, $\psi = -w_{,y}$ in equation (6).

3. SOLUTION TECHNIQUE

The central difference method (CD) is used to solve the system of ordinary differential equations (2). The solution q_{n+1} at time t_{n+1} is computed from formula

$$ q_{n+1} = h^2 M^{-1}(Q_n - R_n) + 2q_n - q_{n-1} \tag{7} $$

where $h = t_{n+1} - t_n$ is the step length. The strain and stress increments are calculated using equations

$$ \Delta E = B_n(q_{n+1} - q_n), \qquad \Delta S = D_n \Delta E $$

The internal force vector at time t_{n+1} is evaluated in accordance with equation (3) using B_{n+1} and $S_{n+1} = S_n + \Delta S$. The initial condition for $\dot{q}_o$ is used to

eliminate q_{-1} in the first step $\dot{q}_o = (q_1 - q_{-1})/2\Delta t$. The CD-scheme with diagonal mass matrix is accurate and simple. As an explicit linear difference method its step length is limited by the largest natural frequency of the finite element mesh.

In the solution of equation (4) the trapezoidal rule or the Newmark scheme with parameters $\gamma = 0.5$ and $\beta = 0.25$ was applied

$$\dot{q}_{n+1} = \dot{q}_n + h\ddot{q}_n/2 + h\ddot{q}_{n+1}/2$$
$$q_{n+1} = q_n + h\dot{q}_n + h^2\ddot{q}_n/4 + h^2\ddot{q}_{n+1}/4 \,. \tag{8}$$

Use of these formulae results in an implicit scheme and therefore iteration has to be used at each time step. The displacement vectors q^i_{n+1} and q^{i+1}_{n+1} in the i^{th} and $(i+1)^{th}$ iteration cycles correspond to configurations 1 and 2 in equation (4). Use of equations (4) and $(8)_2$ yields

$$(K^i_{t,n+1} + 4M/h^2)\Delta q^{i+1} = Q_{n+1} - R^i_{n+1} + M - 4(q^i_{n+1} - q_n)/h^2 + 4\dot{q}_n/h + \ddot{q}_n \,. \tag{9}$$

where $\Delta q^{i+1} = q^{i+1}_{n+1} - q^i_{n+1}$. For the first iteration cycle $q^1_{n+1} = q_n$ is taken. The iteration is continued until $\| \Delta q^{i+1} \| < \varepsilon \| q^{i+1}_{n+1} - q_n \|$ where ε is a tolerance parameter. To account for the drastic changes due to cracking the tangent stiffness K_t was updated in the first iteration cycle but held constant thereafter in order to reduce computing time when using consistent mass matrix.

In Kirchhoff's plate theory a 24 degree of freedom rectangular element was used with 4 nodes and the displacement parameters u, v, w, $w_{,x}$, $w_{,y}$, and $w_{,xy}$ at each node. Integration was performed by 2x2 Gauss quadrature formula. In Mindlin's plate theory 20 and 40 degrees of freedom rectangular elements were employed with 4 and 8 nodes, respectively. The displacement parameters at each node are u, v, w, φ, and ψ. 2x2 Gaussian integration rule was used, exept in case of 20 DOF element only one Gaussian point for the shear deformation. In depthwise direction the integration was carried out by Simpson's rule with 7 integration points. Steel layers were considered separately at their proper places and their effects added to the internal force vector and the tangent stiffness.

4. MATERIAL PROPERTIES

The behaviour of concrete is illustrated by the uniaxial stress-strain diagram in Figure 1. At initial stage, concrete is linearly elastic, isotropic up to the level 30 % of the compressive strength and of the tensile strength. Then plastic strain hardening yield takes place according to a parabolic function. Cracking occurs when a cracking criterion is satisfied. Cracking is brittle and the stress at a discrete crack drops abruptly to zero. The descending part after cracking in Figure 1, however, describes average cracking behaviour over a finite distance and gradual release of tensile stress. In compression, strain softening occurs after the compressive strength in two linear parts, of which the latter corresponds the crushing region.

In multiaxial state of stress the yield criterion is defined as follows

$$F(\sigma, \varepsilon^p) = 3\alpha g^2 J_2 + \beta \bar{\sigma} J_1 + \gamma J_1^2 - \bar{\sigma}^2 = 0 \tag{10}$$

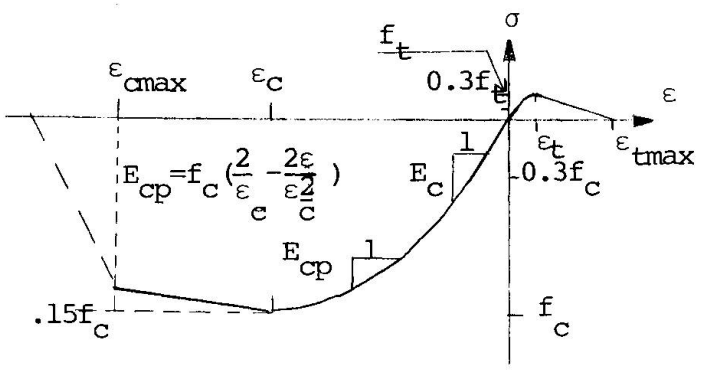

Fig. 1. Uniaxial stress-strain curve of concrete

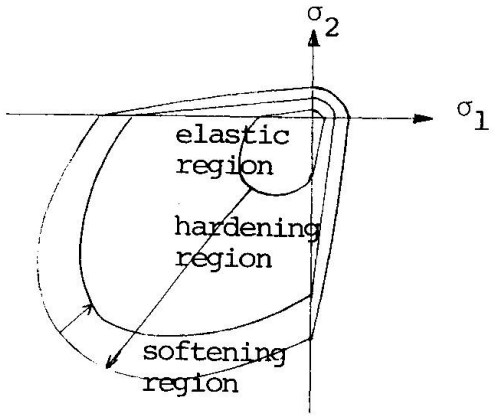

Fig. 2. Biaxial yield and failure criteria of concrete

where J_1 is the first invariant of stress tensor $J_1 = \sigma_{kk}$ and J_2 the second invariant of stress deviator $J_2 = \sigma'_{ij}\sigma'_{ij}/2$. The function

$$g = \delta - (1 - \delta)\cos 3\theta = \delta - (1 - \delta)3\sqrt{3}J_3/2J_2^{3/2} \tag{11}$$

determines the shape of the yield locus in the deviatoric stress plane. J_3 is the third invariant of stress deviator $J_3 = \sigma'_{ij}\sigma'_{jk}\sigma'_{ki}/3$. α, β, γ, and δ are parameters to be determined on the basis of experimental data. The equivalent yield stress $\bar{\sigma}$ is a function of the equivalent plastic strain

$$\bar{\sigma} = \bar{\sigma}(\varepsilon^p), \quad d\bar{\sigma}/d\varepsilon^p = E_p(\varepsilon^p), \quad d\varepsilon^p = (2d\varepsilon^p_{ij}d\varepsilon^p_{ij}/3)^{1/2} \tag{12}$$

It can be obtained from the uniaxial relationship by subtracting the elastic strain. The initial yield stress in equation (10) is $\bar{\sigma} = 0.3\ f_c$. The yield locus expands when $\bar{\sigma}$ increases. Ultimate size is reached when $\bar{\sigma} = f_c$. Parameters α, β, and γ are determined at this stage to fit the experimental results for biaxial stress given in [15]. Using values: $\sigma_1 = -f_c$, $\sigma_2 = 0$; $\sigma_2 = -0.65\ f_c$, $\sigma_1 = -1.25\ f_c$; $\sigma_2 = \sigma_1 = -1.16\ f_c$ one finds for compression-compression region $\alpha = 0.551$, $\beta = -0.872$ and $\gamma = -0.423$, and with values $\sigma_1 = -f_c$, $\sigma_2 = 0$; $\sigma_2 = -0.365\ f_c$, $\sigma_1 = 0.075\ f_c$; $\sigma_2 = 0$, $\sigma_1 = f_t = 0.1\ f_c$ for tension-compression and tension-tension regions $\alpha = 27.49$, $\beta = 7.28$ and $\gamma = -19.22$. In tension-compression and tension-tension regions the ultimate yield locus serves as cracking criterion. Beyond the ultimate yield locus, the softening begins and the yield locus shrinks, see Figure 2. The parameter δ is chosen to be 1.14 in order to keep the yield surface convex.

The associated flow rule is employed. The constitutive equation in plastic flow is accordingly

$$\dot{\sigma} = D_{ep}\dot{\varepsilon} \tag{13}$$

where the elastoplastic constitutive matrix is

$$D_{ep} = C - \frac{C\,n\,n^T\,C}{E_p + n^T\,C\,n} \tag{14}$$

C is the elasticity matrix of concrete. The vector $n \equiv \partial f/\partial\sigma$ is determined on the basis of the yield function (10).

The direction of the crack is taken perpendicular to the maximum tensile stress. After complete cracking concrete behaves uniaxially in the crack direction. The crack is assumed to close when the strain perpendicular to crack direction becomes compressive. After cracking some shear resistance still exists due to aggregate interlocking and dowel action. This is taken into account in reduced shear modulus of concrete [4]

$$G_{red} = \begin{cases} (1 - \varepsilon/\varepsilon_{tmax}) \cdot 0.6 + 0.4\ G, & \varepsilon_t < \varepsilon < \varepsilon_{tmax}, \\ 0.4\ G, & \varepsilon_{tmax} < \varepsilon. \end{cases} \qquad (15)$$

For the steel bars the elastic plastic linearly strain hardening idealization is used. Reinforcement takes axial and shear stresses. Reinforcement is described as smeared uniaxial layers. Complete compatibility between concrete and reinforcement is maintained. The effect of bond slip is taken into account by reducing the modulus of elasticity of reinforcement by 10-20 %.

5. NUMERICAL EXAMPLES

5.1 Statically loaded slabs

Two statically loaded slabs tested by Jofriet & McNeice [3] and Nilsson & Johansson [11] were analyzed numerically and compared with experimental data. In both cases good agreement was obtained.

5.2 Dynamically loaded beam

A freely supported beam tested in [7] was analyzed dynamically. The span, width and thickness of the beam were 2540 mm, 152 mm and 305 mm, respectively. Reinforcement of the beam was 1.23 %. The beam was loaded with a freely falling mass of 1030 kg. The mass time curve was approximated bilinearly. Central deflection vs. time curve is shown in Figure 3.

5.3 Dynamically loaded slabs

A clamped rectangular slab subjected to a jet force at the center is a structure analyzed by Stangenberg [8] using a difference method. In present analysis 2x2 and 3x3 finite element meshes for plate quadrant were used. The calculated time history of the deflection of the central point agrees closely weith the curve given in [8] (Figure 4).

The one way roller supported slab [11] with 2280 mm span, 1230 mm width and 80 mm thickness with reinforcing steel 0.17 % and 0.085 % was tested under a uniformly distributed pressure load varying with time. The central deflection-time history was determined using four isoparametric elements for a plate quadrant (Figure 5).

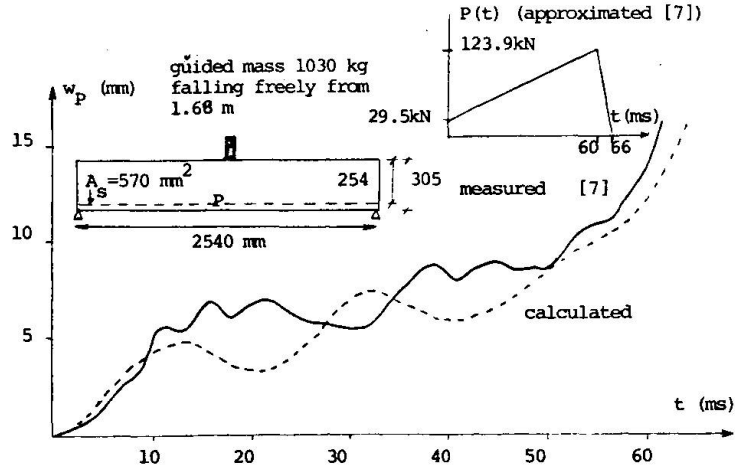

Fig. 3. Midspan deflection vs. time of RC beam, E_c=44 GPa, E_{cp}=100 MPa, f_c=60 MPa, f_t=6 MPa, ν=0.2, ρ=.24E-8Ns^2/mm^4, E_s=210 GPa, E_{sp}=1 GPa, f_s=520 MPa, ν=0.3, 5 elements for half span, time integration by trapezoidal rule.

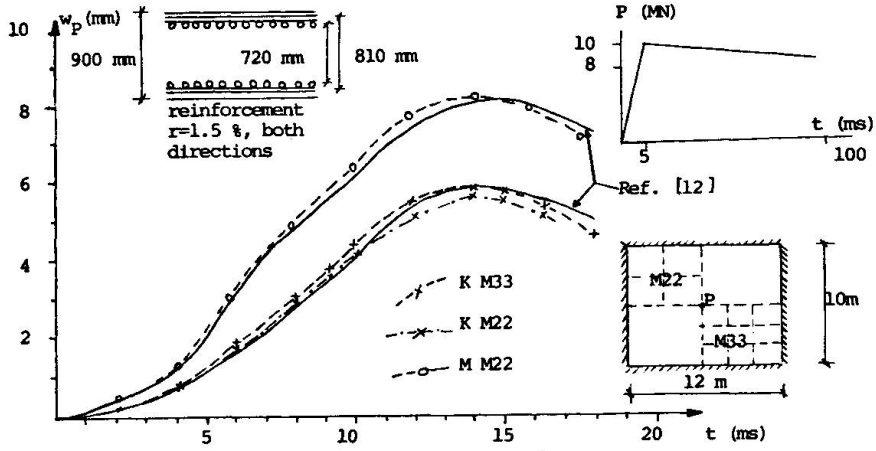

Fig. 4. Deflection vs. time of rectangular plate under central jet force. E_s= 210 GPa, E_c=33 GPa, ν=0.15, f_c=22.7 MPa, f_t=2.27 MPa, f_s=400 MPa, ρ=0.24E-8 Ns^2/mm^4, ε_c=0.002, ε_{cmax}=0.004, ε_t=0.0002, K = Kirchhoff plate theory, M = Mindlin plate theory.

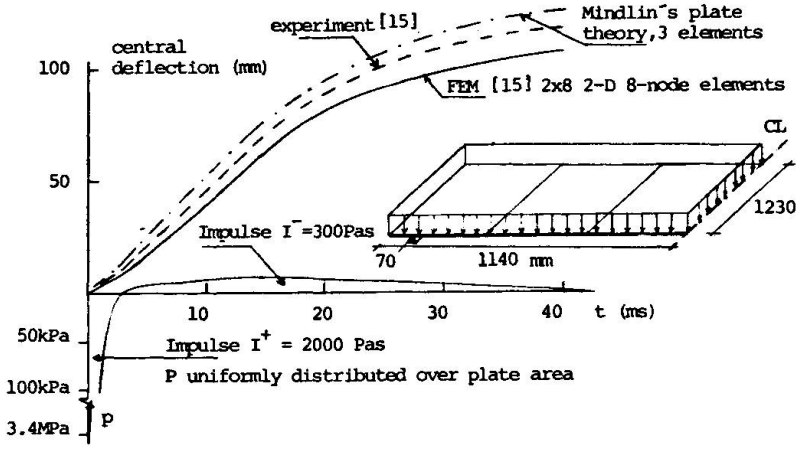

Fig. 5. One way roller supported slab under uniform pressure varying with time. Central deflection vs. time.

6. DISCUSSION

The numerical results obtained for the cases considered indicate that the method describes satisfactorily the behaviour of reinforced concrete slabs at least under static loading. More experimental evidence is needed for dynamic loading. The development of the proposed model is in progress. Systematic study of the factors, viz. cracking, elastic-plastic yield and strain rate effect of concrete, aggregate interlocking, dowel action, etc., affecting the behaviour of reinforced concrete structures and attempts to find realistic simplified models are continued.

REFERENCES

1. MIKKOLA, M.J., and SCHNOBRICH, W.C.: Material Behavior Characteristics for Reinforced Concrete Shells Stresses beyond the Elastic Range. Struct. Res. Series No. 367. University of Illinois. August, 1970.
2. CERVENKA, V.: Inelastic Finite Element Analysis of Reinforced Concrete Panels Under In-Plane Loads. Ph. D. Thesis. University of Colorado, Boulder, 1970.
3. JOFRIET, J.C., and MCNEICE, G.M.: Finite Element Analysis of Reinforced Concrete Slabs. J. Struct. Div., ASCE, Vol. 97, No. ST3, 1971, pp. 785-806.
4. LIN, C.S., and SCORDELIS, A.C.: Nonlinear Analysis of RC Shells of General Form. J. Struct. Div., ASCE, Vol. 101, No. ST3, 1975.
5. SCHNOBRICH, W.C.: Behavior of Reinforced Concrete Structures Predicted by the Finite Element Method. Computers & Structures, Vol. 7, 1977, pp. 365-376.
6. BUYUKOZTURK, O.: Nonlinear Analysis of Reinforced Concrete Structures. Computers & Structures, Vol. 7, 1977, pp. 149-156.
7. NOSSEIR, MOHAMED, S.E.B.: Static and Dynamic Behavior of Concrete Beams Failing in Shear. Ph. D. Thesis. University of Texas, Texas, 1966.
8. STANGENBERG, F.: Nonlinear Dynamic Analysis of Reinforced Concrete Structures. Nucl. Eng. and Design., Vol. 29, No. 1, 1974, pp. 71-88.
9. REBORA, B., ZIMMERMAN, Th., and WOLF, J.P.: Dynamic Rupture Analysis of Reinforced Concrete Shells. Nucl. Eng. and Design. Vol. 37, 1976, pp. 269-.
10. BUYUKOZTURK, O., and CONNOR, J.J.: Nonlinear Dynamic Response of Reinforced Concrete under Impulsive Loading: Research Status and Needs. Nucl. Eng. and Design, Vol. 50, 1978, pp. 83-92.
11. NILSSON, L., and JOHANSSON, I.: Analys med Finit Elementmetod av Luftstötvågsbelastade Enkelspända Betongplattor. FOA Raport C20204-D4, Stockholm, November 1977.
12. NILSSON, L.: Impact Loading on Concrete Structures., Chalmers University of Technology. Publication 79:1. Göteborg 1979.
13. BATHE, K.-J., RAMM, E., and WILSON, E.L.: Finite Element Formulation for Large Deformation Dynamic Analysis. Int. J. Num. Meth. Eng. Vol. 19, 1975, pp. 353-386.
14. HINTON, E., OWEN, D.R.J., and SHANTARAM, D.: Dynamic Transient Linear and Nonlinear Behaviour of Thick and Thin Plates. Mathematics of Finite Elements and Applications (ed. by J.R. Whiteman). Academic Press, 1976, pp. 423-438.
15. KUPFER, H.B., HILSDORF, H.K., and RÜSCH, H.: Behavior of Concrete under Biaxial Stresses. J. of ACI, Vol. 66, No. 8, 1969, pp. 656-666.
16. SCHICKERT, G., and WINKLER, H.: Results of Test Concerning Strength and Strain of Concrete Subjected to Multiaxial Compressive Stresses. Heft 277, Deutscher Ausschuss für Stahlbeton. Berlin 1977.